

A BIOMECHANICAL ANALYSIS OF MUSCLE STRENGTH AS A LIMITING FACTOR IN STANDING POSTURE

ARTHUR D. KUO[†] and FELIX E. ZAJAC

Mechanical Engineering Department, Stanford University, Stanford, CA 94305 USA
and

Rehabilitation R&D Center (153), Veterans Affairs Medical Center, Palo Alto, CA 94304 U.S.A.

Abstract—We developed a method for studying muscular coordination and strength in multijoint movements and have applied it to standing posture. The method is based on a musculoskeletal model of the human lower extremity in the sagittal plane and a technique to visualize, geometrically, how constraints internal and external to the body affect movement. We developed an algorithm to calculate the set of all feasible accelerations (i.e., the 'feasible acceleration set', or FAS) that muscles can induce. For the ankle, knee, and hip joints in the sagittal plane, this set is a polyhedron in three dimensions. Using the volume of the FAS as an indicator of overall mobility, we found that strengthening muscles on the posterior side (as opposed to the anterior) of the body would cause greater increases in mobility. Employing the experimental observations of others, we also found that acceleration constraints greatly reduce the range of feasible accelerations. We then defined a set of four basic acceleration vectors which, when used in various combinations, can produce the repertoire of postural movements. We used linear programming to find the maximum magnitudes of these vectors, and the sensitivity of these magnitudes to muscle strength, thereby delineating those muscles which, if strengthened, would cause the greatest increase in the body's ability to generate the basic acceleration vectors. For our particular model, those muscle groups were found to be hamstrings, tibialis anterior, rectus femoris, and gastrocnemius. These muscle groups would be of great importance in cases involving severely reduced muscle strength. This methodology may therefore be useful for purposes such as design of functional electrical stimulation controllers or exercises for persons at risk for falling.

INTRODUCTION

Muscle strength (peak isometric active-muscle force) obviously places a bound on the performance of many tasks, such as weight-lifting and jumping. However, even in standing, where strength may seem at first not to be a limiting factor, it is indeed reputed to be one factor contributing to loss of balance (e.g. falling in the elderly, Whipple, 1987). In designing functional neuromuscular stimulation control systems to restore function to spinal cord injured persons, decisions must be made as to which muscles to stimulate and how high their force-generating capability needs to be to execute the required tasks.

Task performance is bound, however, not only by the ability of muscles to counteract gravity, but also by their ability to accelerate the body. Since the force produced by a muscle induces acceleration about many joints, including those unspanned by the muscle (Zajac and Gordon, 1989), the upper limit of angular acceleration of any one joint depends on the force-generating capabilities of all the muscles. Moreover, performance of even simple tasks such as posture often involves orchestrated coordination of more than one joint (Nashner and McCollum, 1985). It is natural, therefore, to study not only single joint angular accelerations, but vectors describing the simultaneous angular accelerations of several joints.

At a given instant in time, any coordinated multijoint movement can be completely described by a state vector of positions and velocities and a vector of forces or controls. The vector of joint angular accelerations is a description of the change in the state, and integration of these accelerations is necessary for computation of the state vector. Other researchers, most notably in the field of motor control, have employed vectorial approaches, although usually for single joints with multiple degrees of freedom (van Sonderen *et al.*, 1990; Pellionisz, 1984; Robinson, 1982). Thus, these methods have seen little application to the study of how muscle strength affects multi-joint movement.

In this paper, we shall exclusively use acceleration vectors to describe entire coordination strategies. The coordinated movement of a musculoskeletal system with n pin joints is described by an n -vector, which can conveniently be plotted in n -space. The direction of the n -vector indicates the simultaneous relative movement of all n joints, and the magnitude modulates the size of the accelerations. Unfortunately, acceleration vectors do not provide direct information about the muscular forces that produce movement. This is due to actuator redundancy – there is in general more than one muscle spanning any given joint. By hypothesizing various objective functions, researchers have used optimization principles to resolve such redundancies (cf. An *et al.*, 1984; Bean *et al.*, 1988; Crowninshield and Brand, 1981), providing useful approximations of actual muscle forces.

When studying *maximal* accelerations, however, optimization can rather be used to compute *maximum* theoretical accelerations, which provide upper bounds on

[†]Address correspondence to: Arthur D. Kuo, Design Division, Mechanical Engineering Department, Stanford University, Stanford, CA 94305-4021, U.S.A.

actual accelerations. Therefore, muscles having the greatest effect on these upper bounds, regardless of the objective function used to solve the actuator redundancy problem, can be determined. Indeed, Gordon (1990) proposed using musculoskeletal models to compute the bounds on acceleration as a means to visualize and study muscular synergies and constraints on motion.

Here, we develop an algorithm for the computation of these bounds on acceleration, which define a set ('feasible acceleration set' or FAS) such that the entire set of acceleration vectors achievable by the body is characterized. The size of the FAS serves as a measure of the generalized mobility of the body. The FAS can be used to examine the effect of mechanics, neural and biomechanical constraints, and muscle strength on mobility and the coordination of movement.

We then apply feasible acceleration sets to the study of human posture. Because the FAS corresponding to the body standing unconstrained does not necessarily provide information regarding which of the infinite number of acceleration vectors are relevant to posture, we study how various constraints necessary for upright standing affect the choice of coordination strategies. These constraints reduce the set of serviceable acceleration vectors considerably. A small group of basic acceleration vectors, which can be combined linearly to produce effective coordination strategies in response to postural disturbances, are then definable. We then compute the sensitivity of the maximum magnitude of these accelerations to muscle strength, to determine which muscles limit coordination of postural stability against large disturbances (Kuo and Zajac, 1991a).

While other analyses have dealt with the mechanics of posture (e.g., Gordon, 1990; Nashner and McCollum, 1985), they did not incorporate both musculoskeletal modeling and optimization. We integrate both techniques to develop a methodology for studying coordination of posture and sensitivity to muscle strength.

METHODS

The two main components of this analysis are the musculoskeletal model, and the determination of feasible accelerations based on this model. Together, these are used to study the limits to acceleration vectors, in all directions, as well as in directions dictated by the constraints and mechanics related to control of balance.

Musculoskeletal model

The model of the lower extremity incorporated the dynamics of both the body and of musculotendon actuators (muscle in series with tendon). The body, modeled as a four-segment linkage comprised of the foot, shank, thigh, and head-arms-trunk (i.e., referred to as the 'trunk' hereafter), was assumed to move in the sagittal plane only (Fig. 1) with both sides of the body in postural and load sharing symmetry. The segment lengths and inertial parameters were prescribed for an 'average' adult male (Pandy *et al.*, 1990). The ankle, knee, and hip joints were modeled as simple pin-joints

in the sagittal plane. The equations of motion relating musculotendon actuator forces F^T (a vector in E^m for m muscles) and joint angular accelerations $\ddot{\theta}$ (vector for ankle, knee, and hip joints) are

$$M(\theta)\ddot{\theta} = R(\theta) \cdot F^T + V(\theta, \dot{\theta}) + G(\theta) \quad (1)$$

where M is the mass matrix, R is the matrix of moment arms, V is the vector of velocity-dependent terms, and G is the vector of gravity-dependent terms (see Appendix A). These terms are functions of the joint position vector θ , and V is additionally dependent on the joint angular velocity vector $\dot{\theta}$.

Musculotendon actuators were modeled using a generic Hill-type model, with origin and insertion points determined from musculoskeletal geometry (see Fig. 2; details in Appendix A). The force F_i^T produced by each actuator i is given by

$$F_i^T = F_{oi}^M \cdot F_{li} \cdot F_{vi} \cdot \cos\alpha_i \cdot a_i \quad (2)$$

where F_{oi}^M , F_{li} and F_{vi} describe the peak isometric force, force-length, and force-velocity relationships (see Fig. 3), α_i is the pennation angle, and a_i is the normalized activation level, which is bounded by the inequality

$$0 \leq a_i \leq 1, i=1,2,\dots,m \quad (3)$$

We are confident that this type of model is adequate for simulating human movement. A similar musculoskeletal model has been used to produce simulated jumps that reproduce the salient kinetic, kinematic, and muscle coordination features observed in humans jumping to their maximum achievable heights (Pandy *et al.*, 1990; Pandy and Zajac, 1991).

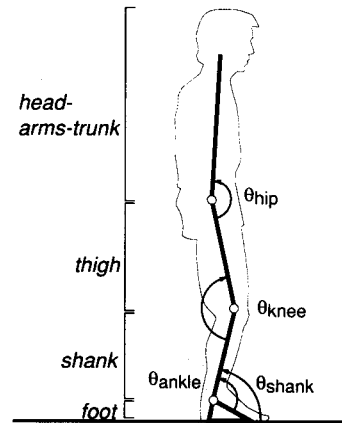


Fig. 1. Three degree-of-freedom planar model of the human body. In joint coordinates, angles are defined to be positive in extension. An additional measurement, the toe angle, is the angle between the floor and the ankle joint, as measured from the toe, and is used to compute toe and heel lift-off constraints. Shank angle is measured clockwise with respect to the horizontal.

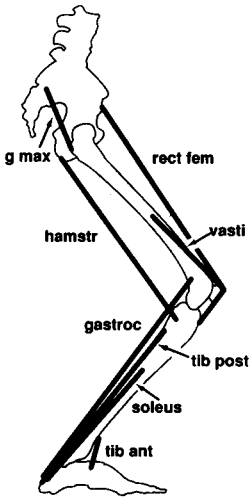


Fig. 2. Schematic of lower extremity showing foot, shank, thigh, and portion of trunk segment. Muscle paths are modeled with three-dimensional locations of origin and insertion points, and in some cases, via points. 33 individual muscles were combined into 14 separate muscle groups dependent on anatomical location. Eight representative muscle groups are shown.

For the study of standing posture, we assumed the motion was quasi-static, i.e., the velocity terms in the dynamical equations, as well as muscle fiber velocities, were small. Thus, the effects of velocity-related terms and the muscle force-velocity relationship were assumed small ($V(\theta, \dot{\theta}) \approx 0$ and $F_v \approx 1$). In addition, muscle activation dynamics were assumed to be slow in relation to the movement speed. Our analysis concerns only selection of acceleration vectors (the set of joint angular accelerations describing movement), and neglects muscle activation sequencing.

The feasible acceleration set

Combining the equations (1) and (2) for the quasi-static condition, we arrive at the equations determining the joint angular acceleration vector $\ddot{\theta}$ (for ankle, knee, and hip joint angular accelerations):

$$\ddot{\theta} = M^{-1}(R \cdot F_o \cdot F_f \cdot a + G) \quad (4)$$

$$= La + g$$

where a is the vector of normalized muscular activation levels, neglecting whether activation is achieved by frequency modulation or recruitment (Stein, 1974). As in equation (1), M is the mass matrix relating torques to angular accelerations and R is the moment arm matrix. F_f and F_o are diagonal matrices characterizing the muscles force-length and maximum isometric force characteristics.

The inequality (3) on normalized activation level of each muscle confines the feasible activations to an m -cube (for $m=14$ muscle groups). Equation (4) is used

to compute the corresponding set of inequalities on the joint angular accelerations $\ddot{\theta}$, transforming the m -cube into a polyhedron in the three-dimensional space defined by ankle, knee, and hip axes (Gordon, 1990). The surface of this polyhedron is the outer bound on all possible accelerations, and we denote its entire volume as the theoretically *feasible acceleration set* (FAS).

This FAS represents all possible body accelerations for a given quasi-static configuration (see Appendix B). Figure 4 shows the FAS for the body in the sagittal plane, for the ankle, knee, and hip joints, in a near-erect standing position. Note that this *ankle-knee-hip FAS* is much longer than it is wide, and wider than it is thick. This indicates that for a given amount of total muscle activation, the corresponding acceleration vectors will have greater magnitudes in some directions than for others. Those vectors with greatest magnitude will be for particular combinations of ankle, knee, and hip movement.

ANALYSIS AND RESULTS

Sensitivity of feasible acceleration set to muscle strength

The larger the volume of the ankle-knee-hip FAS, the greater the set of accelerations possible. The FAS volume can thus be used as an index of the overall mobility of the musculoskeletal system. The volume is given by the formula

$$Volume(FAS) = \sum_{i=1}^m \sum_{j=i+1}^m \sum_{k=j+1}^m \|l_i\| \cdot \|l_j\| \cdot \|l_k\| \cdot |\det[\hat{l}_i, \hat{l}_j, \hat{l}_k]| \quad (5)$$

and the normalized sensitivity to the muscle strength of muscle i is

$$Sensitivity(i) = \frac{\|l_i\|}{Volume(FAS)} \sum_{\substack{j=1 \\ j \neq i}}^m \sum_{\substack{k=j+1 \\ k \neq i}}^m \|l_j\| \cdot \|l_k\| \cdot |\det[\hat{l}_i, \hat{l}_j, \hat{l}_k]| \quad (6)$$

where the vectors l_i are the columns of L in equation (6), split into magnitude $\|l_i\|$ and unit vector \hat{l}_i components (see Appendix B). The normalized sensitivity of mobility can be interpreted as the approximate percentage increase in mobility resulting from a one percent increase in muscle strength. The muscle groups most affecting mobility (i.e., the ankle-knee-hip FAS volume) of the unconstrained body near the upright position are gastroc-nemius, soleus, hamstrings, and gluteus medius/minimus, with sensitivities of about 0.4 to 0.5 (Fig. 5).

Active constraints in standing posture

The ankle-knee-hip FAS defines all possible accelerations of the ankle, knee, and hip joints. However, in standing posture, some of the possible accelerations may be deemed infeasible because they violate certain constraints. To model the task of maintaining stability in

Musculotendon Actuator Model

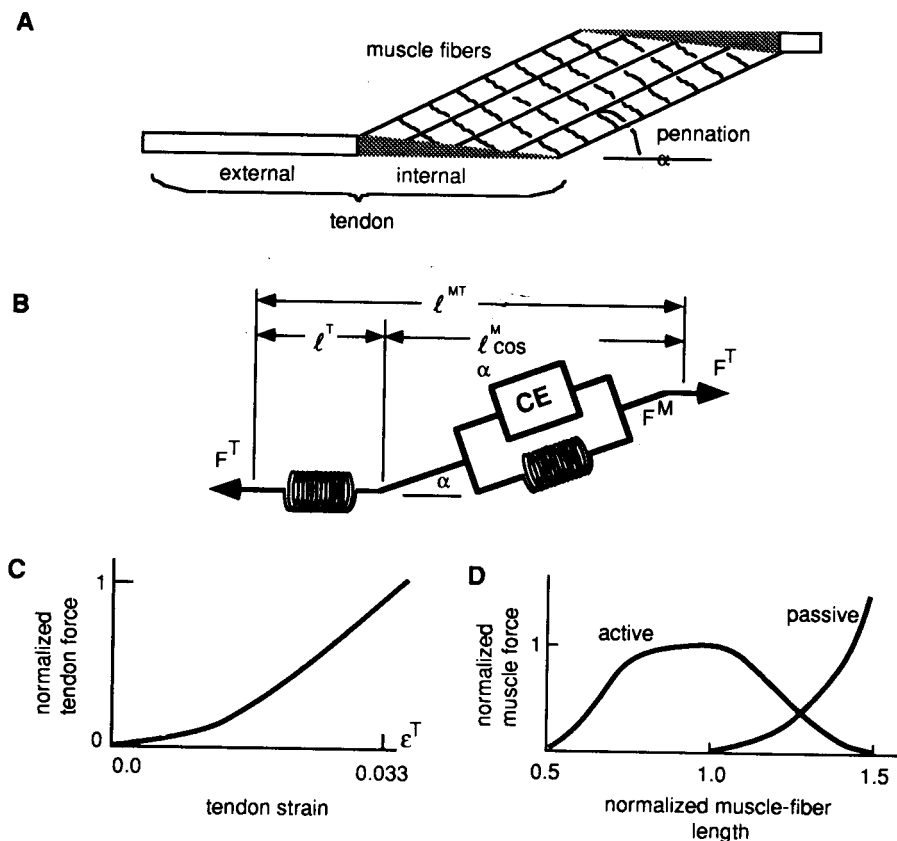


Fig. 3. Musculotendon actuator model. (A) Originating from a skeletal attachment, tendon lies in series with muscle fibers, oriented at a pennation angle α with the tendon. (B) Tendon is represented as a non-linear elastic element, and muscle fibers are represented as an active contractile element in parallel with a passive elastic element. The total musculotendon actuator length ℓ^{MT} is the sum of the muscle-fiber length ℓ^M multiplied by $\cos \alpha$ and the tendon length ℓ^T . (C) Normalized tendon force-length curve. Tendon length is scaled by tendon slack length ℓ_s^T . (D) Normalized muscle force-length curves for active and passive elements. Active muscle force is scaled by activation level a . Muscle and tendon forces are scaled by peak isometric force F_0^M , and muscle fiber length by ℓ_0^M (fiber length where peak active force is developed).

posture, we employed additional constraints on the feasible acceleration sets: keeping the knees straight, keeping the feet flat on the ground, and keeping the center of mass located above the foot.

Human subjects have been found to respond to postural disturbances by moving mostly about the ankles and hips, keeping the knees nearly straight (Nashner and McCollum, 1985). Mathematically, this constraint is enforced in ankle-knee-hip joint angular acceleration space by the *ankle-hip plane* defined by

$$\ddot{\theta}_{kne} = 0. \quad (7)$$

The intersection of this plane with the ankle-knee-hip FAS, called the *ankle-hip FAS*, represents all feasible accelerations while keeping the knees straight.

Since we are concerned with stable posture, we employed additional constraints involved with maintaining stability—keeping the feet flat on the ground. We assumed that either the toes or heels off the ground is a prelude to a less stable configuration. These constraints can be written as

$$c_1^{toe} \ddot{\theta}_{ank} + c_2^{toe} \ddot{\theta}_{kne} + c_3^{toe} \ddot{\theta}_{hip} \geq c_0^{toe} \quad (8)$$

$$c_1^{heel} \ddot{\theta}_{ank} + c_2^{heel} \ddot{\theta}_{kne} + c_3^{heel} \ddot{\theta}_{hip} \geq c_0^{heel} \quad (9)$$

(see Appendix A), and delineate mathematical half-spaces within which the accelerations must be contained. In the ankle-hip plane, these half-spaces are half-planes bounded by lines.

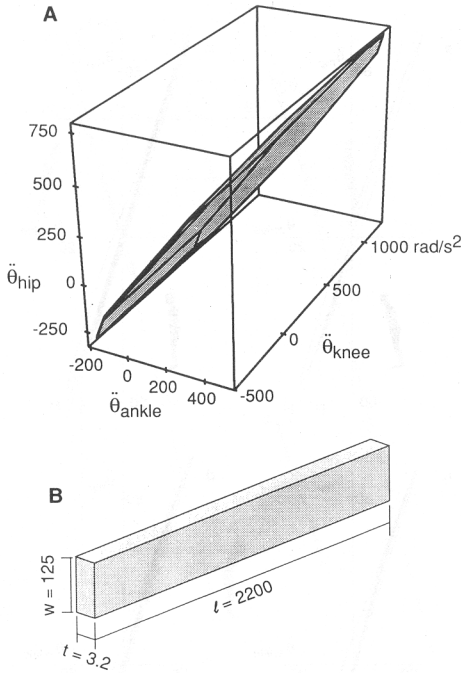


Fig. 4. (A) Ankle-knee-hip Feasible Acceleration Set (FAS) for sagittal plane standing near the upright position. Three axes correspond to joint angular acceleration about the ankle, knee, and hip joints. FAS shows set of all possible combinations of muscle activations. (B) Schematic representation of this FAS indicating approximate length, width, and thickness. Units for (A) and (B) are rad/s².

Another constraint for stable posture is keeping the center of mass located above the foot, that is, keeping its horizontal position between the heels and toes. Once the horizontal location of the center of mass extends beyond the foot, the body cannot exert the appropriate torques to counteract gravity, and cannot remain stable without either receiving an external stabilizing force or taking a step. This constraint acts on body positions, and can be written as (see Appendix A)

$$p_{toe} \leq p(\theta_{ank}, \theta_{kne}, \theta_{hip}) \leq p_{heel} \quad (10)$$

Some accelerations will move the body beyond these position constraints, but only when the body is near them. Thus, when the body is on one of the position boundaries described by a strict equality for equation (10), some accelerations (which will be deemed infeasible) will push the body into an unstable configuration.

Analysis of feasible acceleration sets

When the additional constraints described by equations (7)-(10) are placed upon the ankle-knee-hip FAS, the range of feasible accelerations is greatly reduced, facilitating the study of muscle strength sensitivity to only a few posture-specific acceleration directions. We therefore present here the analysis based on these computations.

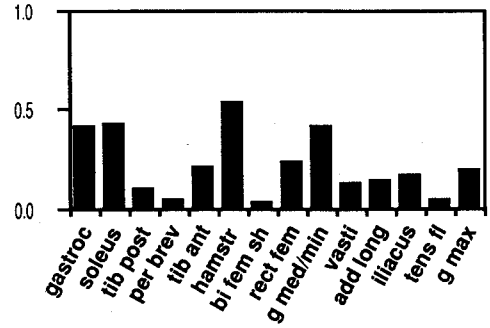


Fig. 5. Sensitivity of mobility (FAS volume) of the ankle-knee-hip FAS to muscle strength. The volume of the ankle-knee-hip FAS (shown in Fig. 4) is taken as an index of the total mobility of the musculoskeletal system. The sensitivity of the mobility index to the strength of each muscle is found by taking partial derivatives of this volume with respect to individual muscle strengths and normalizing.

The *ankle-hip FAS*, from the constraint (7) to keep the knees straight, was computed for four representative positions within the body configuration space (Fig. 6). The four positions correspond to leaning forward to the extremes of stability (Fig. 6a), standing nearly erect in a stable position (Fig. 6b), leaning backward to the extremes of stability (Fig. 6c), and bending forward at the hips in a stable position (Fig. 6d). Fig. 7 shows a close-up of the ankle-hip FAS for each of the four positions, along with the relevant constraints. Note that when leaning forward (Fig. 7a), the center of mass position constraint (10) and flat-footed constraint (9) disallow all but a narrow region of accelerations. Similarly, when leaning backward (Fig. 7c), the center of mass position constraint (10) and flat-footed constraint (8) restrict accelerations conducive to stable posture to a narrow region.

In the more stable near-erect stance (Fig. 7b), the position constraints are not active, and the toe-off and heel-off constraints restrict accelerations to a somewhat larger region. Unlike the sets for forward or backward leaning, however, acceleration vectors in *all* directions are feasible, though those along the flat-footed constraints (as opposed to toward the constraint boundaries) can reach larger magnitude. The feasible accelerations are similar for the bent-forward position (Fig. 7d).

Thus, at the limits of leaning forward or leaning backward, it is necessary to accelerate the hips and ankles in concert in a specific ratio to achieve an acceleration vector that moves the body away the the position boundary (10). Then, once a stance farther from the boundaries is achieved, acceleration vectors in other directions become feasible, and the body can return to erect stance. Experimental observations by others have shown that, for small disturbances, which presumably do not force the body to the position boundaries, human subjects prefer to move primarily about the ankles to maintain erect stance (Horak and Nashner, 1986).

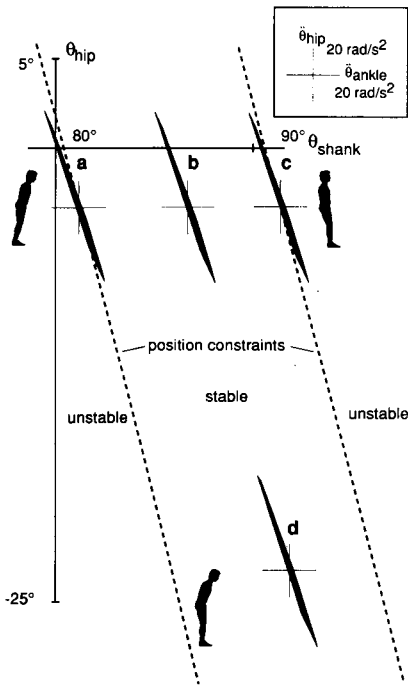


Fig. 6. Ankle-hip (knees motionless, $\dot{\theta}_{knee} = 0$) Feasible Acceleration Sets for four body positions. Dashed lines indicate position boundaries between which the horizontal location of the center of mass can be kept stably between the toes and heels. Each ankle-hip FAS is a polygon because knees are motionless, limiting accelerations to ankle and hip joints (two dimensions). FAS is shown for (a) forward leaning position, (b) near-upright normal stance, (c) backward leaning position, and (d) bent over position, hips flexed. Note that FASs are similar in shape and orientation.

Basic acceleration vectors

Assuming that large postural disturbances must be countered by maximal accelerations, and that smaller disturbances can be countered by submaximal accelerations, we restrict our study to maximal accelerations. The constraints described above restrict the repertoire of stabilizing accelerations sufficiently to facilitate the selection of a group of basic acceleration vectors. These vectors can be summed in linear combinations to produce any desired acceleration vector, with maximal basic acceleration vectors produced by maximal activation of some muscles.

In the ankle-hip plane, any two non-colinear vectors define a basis, meaning that any point in the plane can be expressed as a linear combination of the two basis vectors. Unlike basis vectors, however, basic acceleration vectors, because they are produced by non-negative muscular forces, can only have positive magnitude. Four basic acceleration vectors are therefore required, which can be scaled and combined to produce any feasible acceleration in the ankle-hip plane. At maximum acceleration, the corresponding muscular activation levels, as well as the sensitivity of the maximum acceleration to muscle strength can then be found.

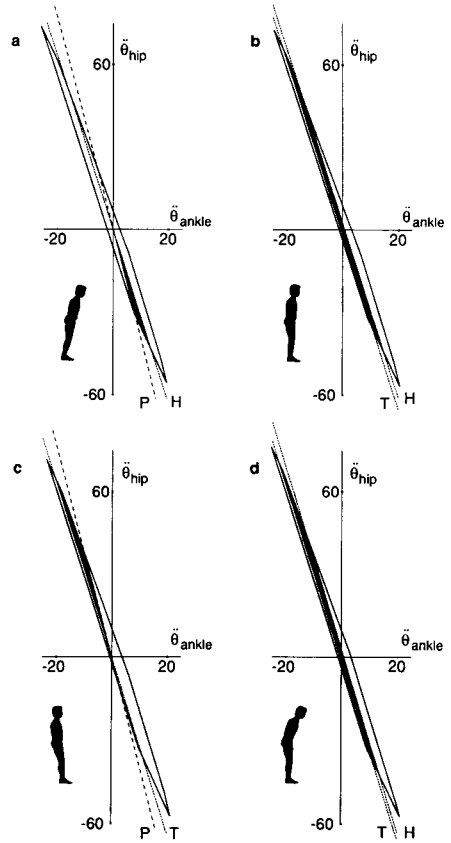


Fig. 7. Ankle-hip Feasible Acceleration Sets for 4 body positions essential to maintenance of stable posture. White polygons delineate those accelerations achievable while keeping the knees straight. Black polygons delineate accelerations satisfying all constraints. (a) When leaning forward (Fig. 6a), accelerations are limited by heel lift-off constraint (dotted line, H) and center-of-mass position constraint (dashed line, P), allowing only simultaneous hip flexion and ankle extension. (b) When in normal standing position, accelerations are limited by heel lift-off (H) and toe lift-off (T) constraints, allowing acceleration in all directions, though those involving ankle extension and hip flexion or vice versa can achieve much greater magnitudes. (c) When leaning backward, accelerations are limited by toe lift-off constraint (T) and center-of-mass position constraint (P), allowing only simultaneous hip extension and ankle flexion. (d) When bent forward at the hip, accelerations are limited by heel lift-off (H) and toe lift-off (T) constraints. Units are in rad/s^2 .

Selection of basic acceleration directions

Each basic acceleration vector is defined by a magnitude and direction. Once its direction is selected, the boundary of the feasible acceleration set determines the maximum magnitude of the vector in that direction. The four basic acceleration directions are chosen by analyzing the ankle-hip FAS corresponding to 3 body positions (Fig. 8a-c). Basic acceleration vector *a* (Fig. 8a) was defined to be along the heel-off constraint (9) so as to accelerate away from the forward position

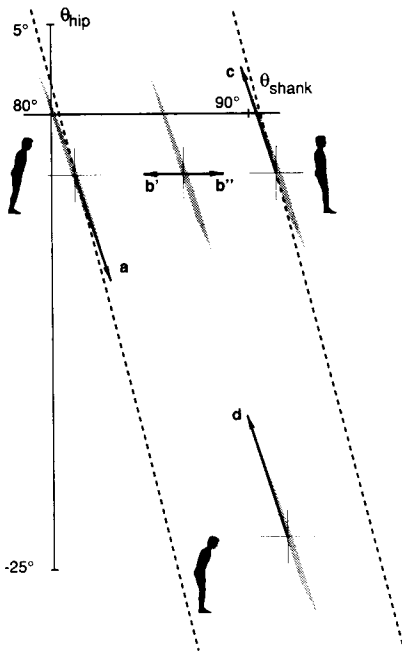


Fig. 8. Ankle-hip ($\dot{\theta}_{knee} = 0$) Feasible Acceleration Sets for four body positions, and basic acceleration directions (arrows). Basic acceleration vectors can be combined to produce the repertoire of postural movements. Directions of basic accelerations are defined as (a) combination of hip flexion and ankle extension from forward leaning, along heel lift-off constraint, similar to the 'hip strategy' of Horak & Nashner (1986); (b' and b'') ankle flexion (extension) in near-erect position, similar to their 'ankle strategy'; and (c) combination of hip extension and ankle flexion from backward leaning, along toe lift-off constraint (hip strategy). An additional direction (d) is defined similar to (c) starting from bent-over position, to study position-dependency of muscle sensitivities. Directions correspond to positions in Figs. 6 and 7.

boundary (Fig. 7a, dotted line). Basic vector *c* (Fig. 8c) was defined to be along the toe-off constraint (8) so as to accelerate away from the backward position boundary (Fig. 7c, dotted line). Basic vectors *b'* (Fig. 8b') and *b''* (Fig. 8b'') were defined to correspond to acceleration about the ankles only, in the forward and backward directions, respectively. Vectors *a* and *c* approximate the 'hip strategy' of Horak and Nashner (1986), while vectors *b'* and *b''* approximate their 'ankle strategy' (Kuo and Zajac, 1991b).

The relative invariance of the ankle-hip FAS in body configuration space (Fig. 6) indicates that these acceleration directions are effective for a wide range of body positions. Nevertheless, for completeness, we also explored an additional acceleration, similar to (Fig. 8c), except starting from a bent over position (Fig. 8d). Such an acceleration would correspond to a straightening motion along the flat-footed constraint (8) through extension of the hips and flexion of the ankles.

Determination of basic acceleration magnitudes

Maximal acceleration along a basic acceleration direction is limited by muscle strength. We wish to find the magnitudes of these accelerations, the corresponding muscle activations, and the sensitivity of these accelerations to muscular strength. Because the constraints and the objective (maximum acceleration) are linear, computation of the maximal accelerations is a linear programming problem and can be written as

$$\min J \quad (11)$$

$$\text{s.t.} \quad Ax = b \quad (12)$$

$$0 \leq x_i \leq 1 \text{ for } i = 1, 2, \dots, m \quad (13)$$

where *x* is the vector of muscular activations; *J*, the objective function, is formulated so as to maximize acceleration in a particular direction; equation (12) constrains movement to the ankle-hip plane and along the particular direction; and equation (13) implements the muscular activation constraints (see Appendix C).

The solution of muscle activations producing a maximum acceleration is not necessarily unique, due to possible redundancies in muscles which need not be maximally activated. For example, a maximum acceleration in a particular direction may require submaximal ankle plantarflexion torque, which can, for example, be distributed non-uniquely between soleus and other plantar flexor muscles. Additional optimization criteria (e.g., Crowninshield and Brand, 1981) may be used to resolve such redundancies. However, maximum acceleration is not sensitive to the strength of those muscles which need not be maximally activated.

Thus, maximal acceleration is only sensitive to the strength of the critical, maximally-activated muscles. The Lagrange multipliers computed during solution of the linear programming problem serve as indicators of the sensitivity, or cost, of maintaining constraints (see Appendix C). To find the sensitivity to muscle strength, the Lagrange multipliers corresponding to equation (13) indicate the cost of a certain maximum activation level against the maximum acceleration objective. Because peak isometric muscle force F_o^M is multiplicative against the activation level, a change in the maximum activation constraint is analogous to a change in F_o^M . Muscles found to have large normalized multipliers would, if strengthened, produce the greatest increase in maximal acceleration for the task.

Analysis of muscular coordination of basic acceleration vectors

Activation levels for the four basic acceleration vectors defined above (along with the additional vector for studying position-dependency) are shown in Fig. 9, left-hand column. For movement of the ankles only (Fig. 9b' and b''), the heel and toe lift-off constraints were chosen to be inactive, so as to show maximum achiev-

able accelerations without moving the knees and hips. These maximum accelerations were found to be 3.2 and 1.2 rad/s² for moving backward and forward, respectively (Fig. 9, middle column). When the heel and toe lift-off constraints (Fig. 7b, dashed lines) are chosen to be active, the body can only accelerate much more slowly (0.92 and 0.45 rad/s², respectively). This demonstrates that the body is capable of accelerating about the ankles approximately 3 times faster than is necessary to lift the toes or heels off the ground.

Normalized sensitivity values for each of the maximal accelerations are given in the right-hand column of Fig. 9. For flexion of the hip and extension of the ankles (Fig. 9a), accelerations are mostly limited by the strength of the hip flexors. Accelerations in the opposite direction (Fig. 9c and d) are, however, not necessarily limited by the hip extensors, but rather by the double-jointed hamstrings, which produce hip extension and knee flexion torques. While activation levels and sensitivities for the two positions (Fig. 9c and d) differ, both share the same high sensitivity to the hamstrings.

DISCUSSION

Coordination of posture

The ankle-knee-hip FAS is highly oriented in a single direction (Fig. 4), indicating that certain combinations of ankle, knee, and hip angular accelerations require less muscular activation than others. The body dynamics mass matrix is relatively close to rank 1, meaning that it is difficult to move the three joints independently. Gordon *et al.* (1988) computed the condition number of the segmental dynamics mass matrix without muscles, and found that the configuration of the body segments is largely responsible for this effect. The ankle-knee-hip FAS demonstrates that the addition of muscles to the model has little effect on this property—the mass matrix remains close to rank 1.

In standing posture, the knees are often kept nearly motionless (Nashner and McCollum, 1985). We have previously found that keeping the knees straight greatly limits vertical acceleration of the center of mass, with little penalty on mobility of the horizontal component of center of mass (Kuo and Zajac, 1991b). Employing this constraint also fosters analysis because feasible accelerations reside in the ankle-hip plane in only two dimensions. In actual standing, some movement of the knees is likely (Allum *et al.*, 1988), but because the ankle-knee-hip FAS is oriented approximately 52° with respect to the knee ($\dot{\theta}_{kne}=0$) plane (Kuo and Zajac, 1991b; see Fig. 4), the feasible ankle-hip accelerations are not highly sensitive to such movement. Should the knees become hyperextended (i.e. mechanical constraints of the knee linkage keep the knee straight), however, muscular forces would no longer be needed to resist extension of the knees. The equations of motion (1) for the three joints used in this analysis here would then be inapplicable. Thus, the muscle coordination patterns found here with the knees slightly flexed may be inappropriate when the knees are hyperextended.

Independent control of just the ankle and hip in the near-upright standing position, with the knees kept stationary through muscular control, is difficult (see ankle-hip FAS, Fig. 6), just as when the knees are allowed to move. The body biomechanics favor hip flexion supplemented with a smaller amount of ankle extension (approximately one-third of the hip acceleration), and vice versa (the hip strategy). The maximum acceleration magnitudes achievable by the hip strategy are at least 20 times larger than for movement about the ankles only (the ankle strategy; compare hip strategy in Fig. 9a, c with ankle strategy, Fig. 9b', b''). This property is virtually independent of body position within the range of upright standing (Fig. 6).

At body positions near the limit of stability, that is, when leaning backward or forward so that the center of pressure is at either the heel or toe, respectively, the constraints (to keep the feet flat on the ground and the center of mass located over the foot) place severe limits on the feasible accelerations. Near a position boundary, any accelerations in the direction of that boundary are likely to cause instability (i.e., horizontal location of center of mass falls outside of heel or toe; see Fig. 7). Also, as the body position nears one of the boundaries, the toe and heel lift-off constraints move as well, further restricting feasible acceleration directions (see Fig. 7). Thus, when the body is at the extremes of forward or backward lean, the hip strategy must be employed.

Based on the size and shape of the constrained feasible acceleration sets, we suggest that four basic acceleration vectors (each specifying relative ankle and hip motion) are sufficient to compose the necessary stabilization strategies to control upright standing. The two hip strategy vectors (Fig. 8a and 8c) and the two ankle strategy vectors (Fig. 8b' and 8b''), can be combined to produce the repertoire of postural strategies. For example, a disturbance pushing the trunk forward close to the position boundary might be countered by a hip strategy flexing the hip and extending the ankles (Fig. 8a), so as to move away from the position boundary while maintaining the feet flat on the ground. As the body moves away from the boundary, the heel-off constraint moves away from the origin, so that the ankles can be extended without lifting the heels. Then, a straightening motion (Fig. 8c) can return the body to an upright position, while ankle flexors are used to brake the motion about the ankle.

These basic acceleration vectors are compatible with the experimentally-based coordination strategies discussed by Horak and Nashner (1986), though our definition of hip and ankle strategies is based on joint angular accelerations rather than electromyograms and force plate records. The analysis presented here, based on the mechanics of the musculoskeletal system, provides a formal mathematical basis for experimental observations of postural movement strategies.

Muscle strength as a limiting factor in standing posture

We postulate that the volume of the feasible acceleration set is an indicator of the overall ability of the

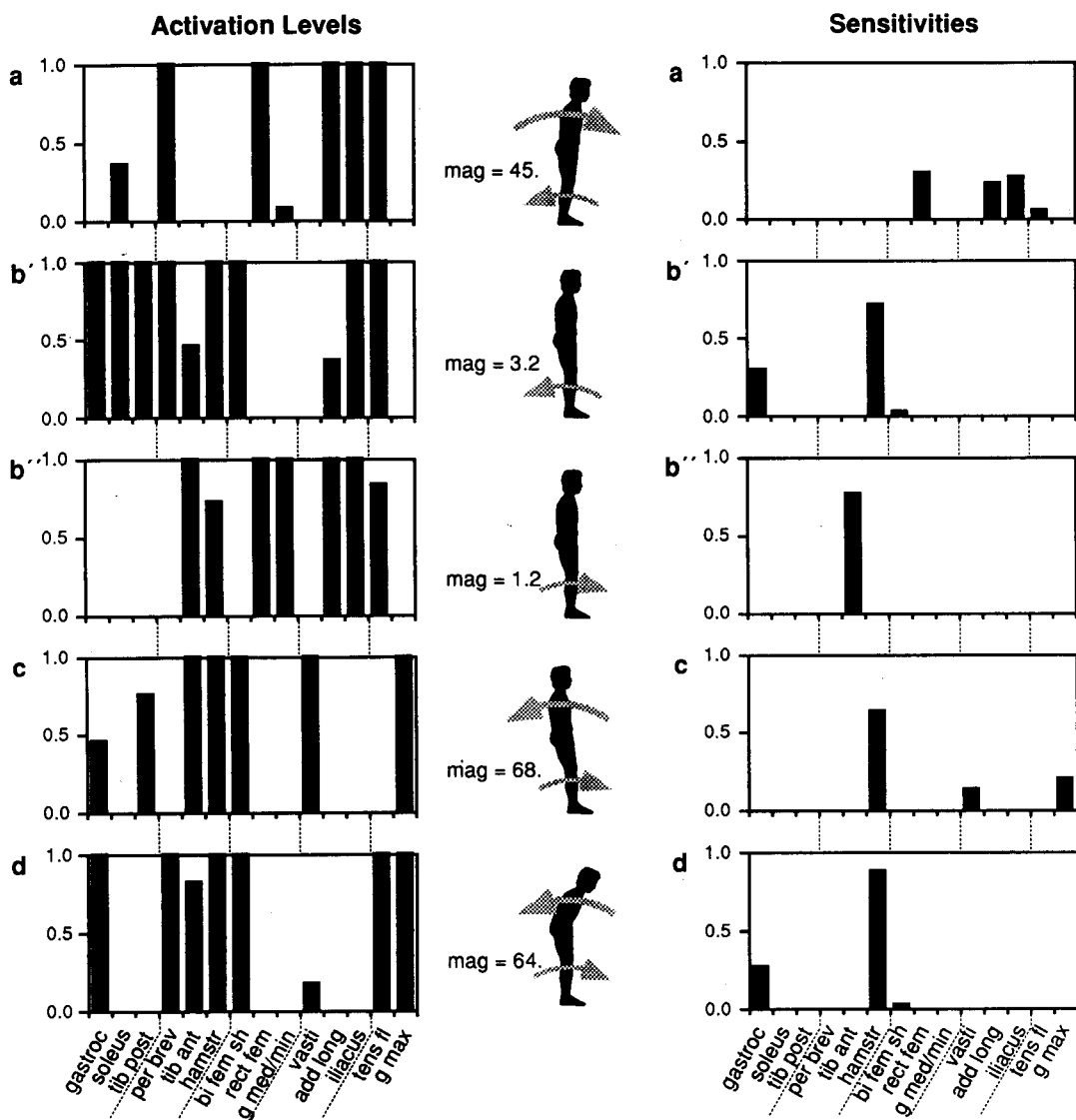


Fig. 9. Activation levels and normalized sensitivities for four basic ankle-hip maximal acceleration vectors (plus one additional vector; see Fig. 8 for acceleration directions), keeping knees motionless. In middle column, icons indicate directions of movement, with magnitudes of acceleration vectors in rad/s^2 . (a) From forward leaning position, flexion of trunk and extension of ankles. (b') From normal position, extension of ankles, keeping other joints motionless. (b'') From normal position, flexion of ankles, keeping other joints motionless. (c) From backward leaning position, extension of hips and flexion of ankles. (d) From bent forward position, extension of hips and flexion of ankles. For all plots, left-hand column shows muscular activation levels solved by linear programming. Right-hand column shows normalized sensitivities computed from the Lagrange multipliers, showing which maximal activation level constraints are most costly. Since maximum isometric force is multiplicative with activation level, another interpretation of these sensitivities is the effect of strengthening of individual muscles. For example, in (d), a 1% increase in hamstring strength would result in approximately 0.9% increase in the magnitude of the maximum acceleration vector, while a similar increase in other muscles such as gluteus maxima would have no such effect.

body to produce accelerations when near the upright standing position. This overall mobility index was found to be most sensitive to the strength of muscles on the posterior side of the body (gastrocnemius, soleus, hamstrings, and gluteus medius/minimus; see Fig. 5). Thus, while knee extensors are necessary to counteract gravity in standing, strengthening of these muscles is a relatively ineffective method of increasing mobility.

Because the ankle and hip strategies can be combined to produce most postural movements, we used linear programming to find the maximal accelerations for these basic acceleration vectors, and their sensitivity to muscle strength. In standing with the knees motionless, we found that sensitivities for the ankle strategy (Fig. 9a and c) are greatest for hamstrings, tibialis anterior, gastrocnemius, and to a lesser degree, biceps femoris (short head). For the hip strategy (Fig. 9b' and b''), we found significant sensitivities for rectus femoris, iliacus, adductor longus, and tensor fascia latae in the forward direction; and for hamstrings, gluteus maximus, and vasti in the backward direction. For both strategies, the hamstring sensitivity is surprising, because it occurs in movements not normally associated with hamstring usage.

The results for some muscles may be exaggerated due to the lack of sophistication in the present musculoskeletal model's pelvis and back musculature. Note also that because the body is capable of producing the ankle strategy (forward and backward) faster than the toe- and heel-off constraints allow, the critical muscles for such movements are only important in cases of greatly reduced muscle strength, such as the elderly. Nevertheless, the results demonstrate that muscles spanning both moving and stationary joints act in concert to produce a movement, and the muscles which limit the speed of the movement may not span the joint undergoing the greatest acceleration.

The sensitivities show the effect of muscle strengthening, regardless of the particular non-unique solution found through linear programming. The Lagrange multipliers are only non-zero for those muscles that are critical for maximal acceleration. Some linear programming solutions may yield maximal activation of some non-critical muscles which need not be fully activated, due to static indeterminacy. Nevertheless, such solutions have no bearing on the sensitivities to critical muscles. For example, the ankle strategy in the backward direction can be achieved with maximum activation of the soleus, tibialis posterior, and peroneus brevis muscle groups (Fig. 9b''). However, none of these groups is critical to maximum acceleration—muscle activation or strength could be reduced in any of the three groups, if combined with a reduction in tibialis anterior activation. The Lagrange multipliers for gastrocnemius, hamstrings, and biceps femoris (short head) muscle groups are non-zero because a change in the strength of any of these muscles will result in a change in maximal acceleration.

Sensitivity of results to modeling parameters

We have found that the basic narrow shape and

orientation of the feasible acceleration sets, which make independent control of joints difficult, are relatively insensitive to assumptions concerning velocity effects or musculoskeletal modeling parameters. Preliminary computations have shown that velocity terms in the equations of motion, which were assumed zero in this study, have little effect on the feasible accelerations. The model will tend to slightly underestimate the magnitude of feasible accelerations under fast eccentric loading conditions, due to the muscle force-velocity relationship. The constraints are dependent on musculoskeletal modeling parameters, but are relatively insensitive to errors. Our qualitative findings utilizing feasible accelerations to study coordination strategies are therefore generalizable to a wide variety of body sizes and types.

The shape and orientation of the feasible acceleration sets are also relatively insensitive to body positions corresponding to stable upright standing (see Fig. 6). However, the muscular coordination pattern for a given movement (e.g., hip strategy, Fig. 8c and 8d) can vary with position. In addition, the critical muscles to which an acceleration vector is sensitive may also vary (see Fig. 9c and 9d).

The current model is confined to movement in the sagittal plane. While the musculoskeletal geometry is modeled in three dimensions, only those muscles which contribute significantly to sagittal plane motion were included. Extension of the model to three dimensions involves inclusion of other muscles and formulating the appropriate equations of motion. However, each additional degree of freedom increases the dimensionality of the feasible acceleration sets, making the system increasingly difficult to analyze.

While our methodology for calculating sensitivity to muscle strength is applicable to many motor tasks, the specific quantitative results are not generalizable to varied body types. The computed maximal accelerations are necessarily specific to the muscle strengths incorporated in the musculoskeletal model; absolute limits on acceleration are only as accurate as the model's parameters. For applications to specific humans, we anticipate the use of these techniques in conjunction with individual-specific modeling methods based on magnetic resonance or other imaging techniques (Delp *et al.*, 1990). These methods can then be used to prescribe muscle strength requirements for performing motor tasks.

Acknowledgements—This work was supported in part by a NSF Pre-Doctoral Fellowship to A.K., NIH grant NS17662 to F.Z., and the Rehabilitation R & D Service, Department of Veterans Affairs.

REFERENCES

- Allum, J.H.J., Keshner, E.A., Honegger, F. and Pfaltz, C.R. (1988) Organization of leg-trunk-head equilibrium movements in normals and patients with peripheral vestibular deficits. In O. Pompeiano and J.H.J. Allum (Eds.), *Vestibulo-spinal Control of Posture and Locomotion, Progress in Brain Research* 76, pp. 277-290, Elsevier, Amsterdam.

- An, K.N., Kwak, B.M., Chao, E.Y. and Morrey, B.F. (1984) Determination of muscle and joint forces: a new technique to solve the indeterminate problem. *J. biomech. Engng.* **106**, 364-367.
- Bean, J.C., Chaffin, D.B., and Schultz, A.B. (1988) Biomechanical model calculation of muscle contraction forces: a double linear programming method. *J. Biomechanics* **21**, 59-66.
- Chao, E. and An, K. (1978) Graphical interpretation of the solution to the redundant problem in biomechanics. *J. biomech. Engng.* **100**, 159-167.
- Chvatal, V. (1983) *Linear Programming* W.H. Freeman, New York.
- Crowninshield, R. and Brand, R. (1981) A physiologically based criterion of muscle force prediction in locomotion. *J. Biomechanics* **14**, 793-801.
- Day, A. M. (1990) The implementation of an algorithm to find the convex hull of a set of three-dimensional points. *ACM Trans. Graphics* **9**, 105-132.
- Delp, S.L., Loan, J.P., Hoy, M.G., Zajac, F.E., Topp, E.L. and Rosen, J.M. (1990) An interactive, graphics-based model of the lower extremity to study orthopaedic surgical procedures. *IEEE Trans. Biomed. Eng.* **37**, 757-767.
- Gordon, M.E., Zajac, F.E., Khang, G., and Loan, J.P. (1988) Intersegmental and mass center accelerations induced by lower extremity muscles: theory and methodology with emphasis on quasi-vertical standing postures. In R.L. Spilker and B. R. Simon (Eds.), *Computational Methods in Bioengineering*, pp. 481-492, American Society of Mechanical Engineers, New York.
- Gordon, M.E. (1990) An Analysis of the Biomechanics and Muscular Synergies of Human Standing. Ph. D. Thesis, Stanford University.
- Horak, F.B. and Nashner, L.M. (1986) Central programming of postural movements: adaptation to altered support-surface configurations. *J. Neurophys.* **55**, 1369-1381.
- Hoy, M.G., Zajac, F.E. and Gordon, M.E. (1990) A musculoskeletal model of the human lower extremity: the effect of muscle, tendon, and moment arm on the moment-angle relationship of musculotendon actuators at the hip, knee, and ankle. *J. Biomechanics* **23**, 157-169.
- Kuo, A.D. and Zajac, F.E. (1991a) A Biomechanical Analysis of Muscle Strength as a Limiting Factor in Human Standing Posture. *Proceedings of the 13th International Congress on Biomechanics*, Perth, West Australia, In press.
- Kuo, A.D. and Zajac, F.E. (1991b) Human standing posture: multijoint movement strategies based on biomechanical constraints. *Progress in Brain Research*, submitted.
- Mantyla, M. (1988) *An Introduction to Solid Modeling*, Computer Science Press, Rockville, Maryland.
- Nashner, L.M. and McCollum, G. (1985) The organization of human postural movements: a formal basis and experimental synthesis. *Behav. Brain Sci.* **8**, 135-172.
- Pandy, M.G., Zajac, F.E., Sim, E. and Levine, W.S. (1990) An optimal control model for maximum-height human jumping. *J. Biomechanics* **23**, 1185-1198.
- Pandy, M.G., Zajac, F.E. (1991) Optimal muscular coordination strategies for jumping. *J. Biomechanics* **24**, 1-10.
- Pellionisz, A. (1984) Coordination: a vector-matrix description of transformations of overcomplete CNS coordinates and a tensorial solution using the Moore-Penrose generalized inverse. *J. Theor. Neurobiol.* **2**, 185-211.
- Preparata, F.P., and Shamos, M.I. (1985) *Introduction to Computational Geometry*, Springer-Verlag, New York.
- Robinson, D.A. (1982) The use of matrices in analyzing the three-dimensional behavior of the vestibulo-ocular reflex. *Biol. Cybern.* **46**, 53-66.
- Rockafellar, R.T. (1970) *Convex Analysis*, Princeton University Press, Princeton.
- Stein, R.B. (1974) Peripheral control of movement. *Physiol. Revs.* **54**, 215-243.
- van Sonderen, J. F. and van der Gon, J. J. D. (1990) A simulation study of a programme generator for centrally programmed fast two-joint arm movements: responses to single- and double-step target displacements. *Biol. Cybern.* **63**, 35-44.
- Whipple, R.L. (1987) Risk factors for falling in the elderly. *J. Amer. Geriatric Soc.* **35**, 13-20.
- Yamaguchi, G.T. and Zajac, F.E. (1989) A planar model of the knee joint to characterize the knee extensor mechanism. *J. Biomechanics* **22**, 1-10.
- Zajac, F.E. (1989) Muscle and tendon: properties, models, scaling, and application to biomechanics and motor control. In J. R. Bourne (Ed.), *Crit. Rev. Biomed. Engng.* **17**, pp. 359-411, CRC Press, Boca Raton.
- Zajac, F.E. and Gordon, M.E. (1989) Determining muscle's force and action in multi-articular movement. In K. Pandolf (Ed.), *Exerc. and Sport Sci. Rev.* **17**, pp. 187-230, Williams and Wilkins, Baltimore.

APPENDIX A: MUSCULOSKELETAL MODEL

Equations of Motion

The equations of motion were derived from Newton's Laws. The relevant parameters of the body segments are:

- m_i = mass of segment i
 I_i = moment of inertia of segment i about its center of mass
 l_i = length of segment i
 l_{ci} = distance from distal joint to mass center of segment i

(assuming that each segment's mass center lies along the line connecting the joints) for the foot, shank, thigh, and head-arms-trunk, which we use to define the following symbols:

$$\begin{aligned} c_1 &= m_1 l_{c1} + (m_2 + m_3 + m_4) l_1 \\ c_2 &= m_2 l_{c2} + (m_3 + m_4) l_2 \\ c_3 &= m_3 l_{c3} + m_4 l_3 \\ c_4 &= m_4 l_{c4} \\ a_{11} &= I_1 + m_1 l_{c1}^2 + (m_2 + m_3 + m_4) l_1^2 \\ a_{12} &= c_2 l_1 \\ a_{13} &= c_3 l_1 \\ a_{14} &= c_4 l_1 \\ a_{22} &= I_2 + m_2 l_{c2}^2 + (m_3 + m_4) l_2^2 \\ a_{23} &= c_3 l_2 \\ a_{24} &= c_4 l_2 \\ a_{33} &= I_3 + m_3 l_{c3}^2 + m_4 l_3^2 \\ a_{34} &= c_4 l_3 \\ a_{44} &= I_4 + m_4 l_{c4}^2 \end{aligned}$$

With the joint angles defined in Fig. 1 and the additional angle θ_{ine} defined by the ankle joint, toe (MCP) joint, and heel, we add the following symbols:

$$\begin{aligned} M_{01} &= -(a_{22} + a_{33} + a_{44} \\ &\quad + a_{12} \cos(\pi - \theta_{ank}) + a_{13} \cos(-\theta_{ank} + \theta_{kne}) \\ &\quad + a_{14} \cos(\pi - \theta_{ank} + \theta_{kne} - \theta_{hip}) + 2a_{23} \cos(\pi - \theta_{kne}) \\ &\quad + 2a_{24} \cos(\theta_{hip} - \theta_{kne}) + 2a_{34} \cos(\pi - \theta_{hip})) \\ M_{02} &= a_{33} + a_{44} + a_{13} \cos(-\theta_{ank} + \theta_{kne}) + a_{14} (\pi - \theta_{ank} + \theta_{kne} - \theta_{hip}) \\ &\quad + a_{23} \cos(\pi - \theta_{kne}) + a_{24} \cos(\theta_{hip} - \theta_{kne}) + 2a_{34} \cos(\pi - \theta_{hip}) \\ M_{03} &= -(a_{44} + a_{14} \cos(\pi - \theta_{ank} + \theta_{kne} - \theta_{hip}) \\ &\quad + a_{24} \cos(\theta_{hip} - \theta_{kne}) + a_{34} \cos(\pi - \theta_{hip})) \\ M_{11} &= a_{22} + a_{33} + a_{44} + 2a_{23} \cos(\pi - \theta_{kne}) + 2a_{24} \cos(\theta_{hip} - \theta_{kne}) \\ &\quad + 2a_{34} \cos(\pi - \theta_{hip}) \\ M_{12} &= -(a_{33} + a_{44} + a_{23} \cos(\pi - \theta_{kne}) + a_{24} \cos(\theta_{hip} - \theta_{kne}) \\ &\quad + 2a_{34} \cos(\pi - \theta_{hip})) \\ M_{13} &= a_{44} + a_{24} \cos(\theta_{hip} - \theta_{kne}) + a_{34} \cos(\pi - \theta_{hip}) \\ M_{22} &= a_{33} + a_{44} + 2a_{34} \cos(\pi - \theta_{hip}) \\ M_{23} &= -(a_{44} + a_{34} \cos(\pi - \theta_{hip})) \\ M_{33} &= a_{44} \end{aligned}$$

$$G_0 = (c_1 \cos(\pi - \theta_{ioe}) + c_2 \cos(\theta_{ank} - \theta_{ioe}) + c_3 \cos(\pi - \theta_{ioe} + \theta_{ank} - \theta_{kne}) + c_4 \cos(-\theta_{ioe} + \theta_{ank} - \theta_{kne} + \theta_{hip}))g$$

$$G_1 = -(c_2 \cos(-\theta_{ioe} + \theta_{ank}) + c_3 \cos(\pi - \theta_{ioe} + \theta_{ank} - \theta_{kne}) + c_4 \cos(-\theta_{ioe} + \theta_{ank} - \theta_{kne} + \theta_{hip}))g$$

$$G_2 = (c_3 \cos(\pi - \theta_{ioe} + \theta_{ank} - \theta_{kne}) + c_4 \cos(-\theta_{ioe} + \theta_{ank} - \theta_{kne} + \theta_{hip}))g$$

$$G_3 = -(c_4 \cos(-\theta_{ioe} + \theta_{ank} - \theta_{kne} + \theta_{hip}))g$$

$$V_0 = \theta_{ank}^2 (a_{12} \sin(\pi - \theta_{ank}) + a_{23} \sin(\pi - \theta_{kne}) + a_{24} \sin(\theta_{kne} - \theta_{hip})) - (\theta_{ank} - \theta_{kne})^2 (a_{13} \sin(\theta_{ank} - \theta_{kne}) + a_{23} \sin(\pi - \theta_{kne}) + a_{34} \sin(\pi - \theta_{hip})) + (\theta_{ank} - \theta_{kne} + \theta_{hip})^2 (a_{14} \sin(\pi - \theta_{ank} + \theta_{kne} - \theta_{hip}) + a_{24} \sin(\theta_{kne} - \theta_{hip}))$$

$$V_1 = -\theta_{ank}^2 (a_{23} \sin(\pi - \theta_{kne}) + a_{24} \sin(\theta_{kne} - \theta_{hip})) + (\theta_{ank} - \theta_{kne})^2 (a_{23} \sin(\pi - \theta_{kne}) + a_{34} \sin(\pi - \theta_{hip})) - (\theta_{ank} - \theta_{kne} + \theta_{hip})^2 (a_{24} \sin(\theta_{kne} - \theta_{hip}) + a_{34} \sin(\pi - \theta_{hip}))$$

$$V_2 = \theta_{ank}^2 (a_{23} \sin(\pi - \theta_{kne}) + a_{24} \sin(\theta_{kne} - \theta_{hip})) - (\theta_{ank} - \theta_{kne})^2 (a_{34} \sin(\pi - \theta_{hip})) + (\theta_{ank} - \theta_{kne} + \theta_{hip})^2 (a_{34} \sin(\pi - \theta_{hip}))$$

$$V_3 = -\theta_{ank}^2 (a_{24} \sin(\theta_{kne} - \theta_{hip})) + (\theta_{ank} - \theta_{kne})^2 (a_{34} \sin(\pi - \theta_{hip}))$$

$$F_{\theta 1} = c_2 \cos(\pi - \theta_{ioe}) + c_3 \cos(\pi - \theta_{ioe} + \theta_{ank} - \theta_{kne}) + c_4 \cos(-\theta_{ioe} + \theta_{ank} - \theta_{kne} + \theta_{hip})$$

$$F_{\theta 2} = c_3 \cos(\pi - \theta_{ioe} + \theta_{ank} - \theta_{kne}) + c_4 \cos(-\theta_{ioe} + \theta_{ank} - \theta_{kne} + \theta_{hip})$$

$$F_{\theta 3} = c_4 \cos(-\theta_{ioe} + \theta_{ank} - \theta_{kne} + \theta_{hip})$$

$$F_{\theta} = \theta_{ank}^2 (c_2 \sin(\pi - \theta_{ioe}) + c_3 \sin(\pi - \theta_{ioe} + \theta_{ank} - \theta_{kne}) + c_4 \sin(-\theta_{ioe} + \theta_{ank} - \theta_{kne} + \theta_{hip}))$$

$$+ (\theta_{ank} - \theta_{kne})^2 (c_3 \sin(\pi - \theta_{ioe} + \theta_{ank} - \theta_{kne}) + c_4 \sin(-\theta_{ioe} + \theta_{ank} - \theta_{kne} + \theta_{hip}))$$

$$+ (\theta_{ank} - \theta_{kne} + \theta_{hip})^2 (c_4 \sin(-\theta_{ioe} + \theta_{ank} - \theta_{kne} + \theta_{hip}))$$

$$F_G = g(m_1 + m_2 + m_3 + m_4)$$

The matrices and vectors required for equation (1) are found based on the symbols above:

$$M = \begin{bmatrix} M_{11} & M_{12} & M_{13} \\ M_{12} & M_{22} & M_{23} \\ M_{13} & M_{23} & M_{33} \end{bmatrix}$$

$$V = [V_1 \quad V_2 \quad V_3]'$$

$$G = [G_1 \quad G_2 \quad G_3]'$$

where A' refers to the transpose of A .

To compute the constraints for toe and heel lift-off, we find the ground reaction forces acting on the foot, and compute the resultant ground reaction force and torque acting about an arbitrary point on the foot. For example, we use equations for a four degree-of-freedom linkage to find the resultant ground reaction torque about the toe, T_{ioe} :

$$M_{01} \theta_{ank} + M_{02} \theta_{kne} + M_{03} \theta_{hip} = G_0 + V_0 + T_{ioe} \quad (A1)$$

The resultant ground reaction force at the toe is

$$F_{gr} = F_{\theta}' \theta + F_{\theta} + F_G \quad (A2)$$

where $F_{\theta} = [F_{\theta 1} \quad F_{\theta 2} \quad F_{\theta 3}]'$.

If this resultant ground reaction force is moved to the heel, we can compute the corresponding ground reaction torque about the heel, T_{hl} , with

$$T_{hl} = -T_{ioe} + F_{gr} l_f \quad (A3)$$

where l_f is the length of the foot between the toe joint and the heel.

The constraints are that the ground reaction torques at the toes and heels are both positive, meaning that the heels and toes are supported by the ground:

$$T_{ioe} \geq 0 \quad (A4)$$

$$T_{hl} \geq 0 \quad (A5)$$

Combining equations (A1), (A2), (A3), (A4), and (A5), we can find constraints in the form of equations (8) and (9):

$$M_0' \theta \geq G_0 + V_0 \quad (A6)$$

$$(F_{\theta}' l_f - M_0') \theta \geq -(G_0 + V_0 + F_{\theta} l_f + F_G l_f) \quad (A7)$$

where M_0 is a vector of the M -symbols of equation (A1). Note that we assume the velocity effects in V_0 are negligible in our current model.

In order to form the constraints on body position so as to keep the center of mass located above the foot, we use the same equations above, except that the system is in static equilibrium. Setting $\dot{\theta} = 0$ in equations (A1) and (A2), we substitute into equations (A3), (A4), and (A5) to find a relation in the joint angles θ that can be put in the form of equation (10).

Musculoskeletal Geometry

The musculoskeletal geometry dictates the paths, and therefore the moment-generating capabilities of the muscles. We modeled the path of each musculotendon actuator with a series of straight lines going through points of origin, insertion, and, if necessary, via points (Hoy *et al.*, 1990; Delp *et al.*, 1990). Figure 2 shows a diagram of the paths of some sample muscles. A kinematic model was used to characterize the moment arms about the knee (Yamaguchi and Zajac, 1989; Delp *et al.*, 1990). This model facilitated the computation of the length of each musculotendon actuator ℓ_i^{MT} , and from that, the moment arm matrix of equation (1):

$$R(\theta)' = \frac{\partial \ell^{MT}}{\partial \theta} \quad (A8)$$

Musculotendon Actuators

Musculotendon actuator function was characterized by a generic Hill-type model comprised of tendon in series with muscle fibers (Zajac, 1989) and scaled by four actuator-specific parameters: pennation angle α , tendon slack length ℓ_s^T , peak isometric force F_0^M , and optimal muscle-fiber length ℓ_0^M . Tendon is oriented at a pennation angle α with respect to the muscle fibers (see Fig. 3a), and is modeled as a nonlinear elastic element with force developing only at lengths exceeding the tendon slack length, ℓ_s^T . The muscle is characterized by a passive elastic element in parallel with an active contractile element, as depicted in Fig. 3b. Each element produces force according to a normalized force-length curve (passive and active) scaled by optimal muscle-fiber length ℓ_0^M . In addition, the active element is modulated by a force-velocity relationship. Tendon develops force according to its own force-strain curve (Fig. 3c and d). These forces are scaled by peak isometric muscle force F_0^M . The active muscle force is also scaled by a multiplication with the activation level,

$$0 \leq a_i \leq 1, \quad i=1,2, \dots, m \quad (A9)$$

The muscle force for an individual muscle i can be written as

$$F_i^M = F_{0i}^M \cdot F_{\ell i} \cdot F_{v i} \cdot a_i \quad (A10)$$

where $F_{\ell i}$ characterizes the force-length relationship and $F_{v i}$ characterizes the force-velocity relationship.

We grouped 33 lower-extremity musculotendon actuators into 14 muscle groups based on anatomical position (e.g., ankle dorsiflexors, hamstrings, vasti; see Table A1). For simplicity, the muscles within each of the 14 muscle groups were assumed to share common activation commands from the nervous system. Maximum isometric force achievable at a specific musculotendon length was computed through an iterative

procedure to reach a static equilibrium between the muscle and tendon elements (Delp *et al.*, 1990)

$$F^T = F^M \cos \alpha \quad (A11)$$

Table A1. Muscle groups incorporated in musculoskeletal model

Muscle group	Description
gastroc soleus	gastrocnemius, lateral and medial heads
tib post	soleus
	tibialis posterior, flexor dig. longus, flexor hal. longus
per brev	peroneus brevis, peroneus longus
tib ant	tibialis ant., peroneus tertius, ext. dig. longus, ext. hal. longus
hamstr	semimembranosus, semitendinosus, biceps femoris (long head)
bi fem sh	biceps femoris (short head)
rect fem	rectus femoris
g med/min	gluteus medius and minimus, 2 parts each
vasti	vastus medius, intermedius, lateralis
add long	adductor longus, adductor brevis, pectineus
iliacus	iliacus, psoas
tens fl	tensor fasciae latae
g max	gluteus maximus, 3 parts

APPENDIX B: THE FEASIBLE ACCELERATION SET

The boundary of the feasible acceleration set (FAS) is the convex hull of the affine transformation of a hypercube. For the case of standing posture in the sagittal plane, the transformation is from m -space (for m muscles) to 3-space (for ankle, knee, and hip joint angular accelerations). There exist general algorithms for the evaluation of convex hulls, but these algorithms typically have theoretical worst-case complexity of $O(n \log n)$ (Preparata and Shamos, 1985). In actual implementation, they appear to exhibit worst-case complexity of $O(n^2)$ (Day, 1990). The hypercube describing the set of allowable muscle activations has 2^m vertices, so that a general convex hull algorithm may operate on $O(4^m)$. To make computation more efficient, we designed a simple algorithm to take advantage of the original hypercube structure of the vertices undergoing transformation to construct the FAS from a recursive definition.

We define the following operations on convex sets (Rockafellar, 1970): The sum of two sets in m -space

$$M = M_1 + M_2 \quad (B1)$$

is

$$M = \{ x \in E^m \mid x = x_1 + x_2, x_1 \in M_1, x_2 \in M_2 \} \quad (B2)$$

The linear mapping of a set in m -space to n -space is defined as

$$LM_1 = \{ x \in E^n \mid x = Ly \forall y \in M_1 \} \quad (B3)$$

where $L \in E^{n \times m}$. Note that both operations produce convex sets (Rockafellar, 1970).

We also define the set of allowable activations for each individual muscle

$$a_i \equiv \{ x \in E^m \mid x = \lambda_i e^i, 0 \leq \lambda_i \leq 1 \} \text{ for } i=1, 2, \dots, m \quad (B4)$$

where e^j are standard basis vectors in Euclidean space E^m : $e^1 = [1 \ 0 \ 0 \ \dots \ 0]^T$, $e^2 = [0 \ 1 \ 0 \ \dots \ 0]^T$, ..., $e^m = [0 \ 0 \ 0 \ \dots \ 1]^T$.

From this definition, we can define the m -cube of all allowable muscle activations using j muscles:

$$C^j \equiv \left\{ x \in E^m \mid x = \sum_{i=1}^j a_i \right\} \text{ for } j = 1, 2, \dots, m \quad (B5)$$

The feasible acceleration set F is in the form of an affine transformation of C^m :

$$F = LC^m + v \quad (B6)$$

and we define the smaller sets

$$F^j \equiv LC^j \text{ for } j = 1, 2, \dots, m \quad (B7)$$

so that F is found from

$$F = F^m + v \quad (B8)$$

Noting from definition (B5) above that

$$C^{j+1} = C^j + a_{j+1} \text{ for } j = 1, 2, \dots, m-1 \quad (B9)$$

we arrive at the equations

$$\begin{aligned} F^{j+1} &= LC^{j+1} \\ &= LC^j + La_{j+1} \\ &= F^j + La_{j+1} \end{aligned} \quad (B10)$$

Thus F can be found simply through the addition of convex polytopes.

To efficiently implement this definition in an algorithm, we chose a subset of the full winged-edge data structure for description of the polytope surface (Mantyla, 1988). The algorithm first determines the dimension $d = \text{rank}(L)$ of the feasible acceleration set, and then selects d muscles and numbers them a_i ($i=1, 2, \dots, d$) such that La_i spans d dimensions. From this basic d -polytope, designated F^d , we can use equation (B10) to construct F . As each muscle La_{j+1} is included, certain faces, edges, and vertices of F^j become interior in F^{j+1} , and are deleted from the surface data structure. The data structure is well-suited for such operations, and is also convenient for computing intersections of F with constraints.

This algorithm exhibits empirical complexity of approximately $O(1.4^m)$. While not exceptional, this complexity is nevertheless much more practical than that of a more general convex hull algorithm.

Computation of Feasible Acceleration Set Volume

Denote the columns of the mapping matrix L of equation (B6) by l_i , $i=1, 2, \dots, m$. Consider the case in which all columns are non-colinear. As each muscle La_{i+1} is added as described above, a parallelepiped is added to each face of the partial polytope LC^i that faces within 90 degrees of the vector l_{i+1} . Thus, the final feasible acceleration set has volume equal to the sum of the volumes of each of the parallelepipeds.

This volume can be computed by breaking the columns l_i into two components: magnitude $\|l_i\|$ and unit vector \hat{l}_i . Then the volume is

$$\text{Volume}(FAS) = \sum_{i=1}^m \sum_{j=i+1}^m \sum_{k=j+1}^m \|l_i\| \cdot \|l_j\| \cdot \|l_k\| \cdot |\det[\hat{l}_i, \hat{l}_j, \hat{l}_k]| \quad (B11)$$

The sensitivity of this volume to changes in the maximum isometric force F_0^M of any muscle is simply the partial derivative of the volume with respect to the magnitude $\|l_i\|$ which is multiplicative against F_0^M [see equation (4)]. We normalize this derivative with respect to the size of the volume and $\|l_i\|$:

$$\text{Sensitivity}(i) = \frac{W_i}{\text{Volume}(FAS)} \sum_{\substack{m \\ j=1}} \sum_{\substack{m \\ j=1}} W_j \cdot W_k \cdot |\det[\hat{i}_i, \hat{i}_j, \hat{i}_k]| \quad (\text{B12})$$

For the more general case in which some columns may be colinear, colinear sets of columns may be combined together until all columns are non-colinear, and recognize that this has no effect on the volume of the feasible acceleration set.

APPENDIX C: LINEAR PROGRAMMING

To formulate the linear programming problem, we recognize that we wish to find the maximum accelerations possible along a certain set of constraints. The joint angular accelerations can be written as an affine transformation of the muscular activation inputs $x = [a_1, a_2, \dots, a_3]'$:

$$\ddot{\theta} = Lx + v \quad (\text{C1})$$

The constraint to keep the knees straight, equation (9), is simply

$$c^{kne'} x = c_0^{kne} \quad (\text{C2})$$

where $c^{kne} = [0 \ 1 \ 0]'$, $c_0^{kne} = 0$.

For a given acceleration, only one of the toe or heel constraints, Equations (10) and (11) will be active. Designating the active constraint as c^* , we find its normal vector in the ankle-hip plane

$$n = [c_j^*, 0, -c_l^*]' \quad (\text{C3})$$

where the second element is 0 because constraint (C2) already ensures a solution in the ankle-hip plane.

The problem is then

$$\min_x J = \pm n' Lx \quad (\text{C4})$$

$$\text{s.t. } Ax = b \quad (\text{C5})$$

$$0 \leq x_i \leq 1 \text{ for } i=1,2, \dots, m \quad (\text{C6})$$

where the sign of equation (C4) is dependent on the direction we wish to find the extreme in, and the constraints are combined into

$$A = \begin{bmatrix} c^{kne'} L \\ c^{*'} L \end{bmatrix}, \quad b = \begin{bmatrix} c_0^{kne} - c^{kne'} v \\ c_0^* - c^{*'} v \end{bmatrix}. \quad (\text{C7})$$

In optimization problems, constraints c^* are often adjoined to the objective function in the manner of

$$\min_x J = \pm n' Lx + \lambda c^* \quad (\text{C8})$$

where c^* is an equality ($c^* = 0$) or inequality ($c^* \leq 0$) constraint and λ is the Lagrange multiplier.

Optimization theory guarantees that for inequality constraints, at the optimal value of x ,

$$\lambda \geq 0 \quad (\text{Chvatal, 1983}). \quad (\text{C9})$$

Note that the multiplier satisfies the equation

$$\lambda = \frac{\partial J}{\partial c^*}. \quad (\text{C10})$$

and can be interpreted as the sensitivity of the objective function to the constraint. If we consider the constraint to the maximum muscle activation input, which is multiplicative against the peak isometric force F_0^M , the Lagrange multiplier can be interpreted as the sensitivity of the maximum acceleration to either maximum muscle activation or peak isometric force. We then normalize this value by dividing by the optimal value of J . This procedure is then carried through for the multiplier for each of the activation level constraints.